JOURNAL OF CATALYSIS 69, 445–453 (1981)

Concentration Profiles and the Design of Metal-Supported Catalysts

S. S. KULKARNI, G. R. MAUZE, AND J. A. SCHWARZ

Department of Chemical Engineering and Materials Science, Syracuse University, Syracuse, New York 13210

Received September 8, 1980; revised January 5, 1981

Theoretical results (R. C. Vincent and R. P. Merrill, *J. Catal.* **35**, 206 (1974)) have shown that it is possible to describe the concentration profile of catalytic metals within a macroporous catalyst support prepared by the incipient wetness technique. However, most catalysts are prepared under conditions where a coingredient is present in the impregnating solution. If the design of desired concentration profiles is to be successful, the earlier model proposed must be extended to include competing coingredients during the impregnation process. This report offers such an extension by considering two species competing for surface sites on the support during impregnation. For adsorption obeying Langmuir kinetics, the critical parameters which determine the profiles for each of the adsorbed species have been identified. However, attempts to fit the recent studies of Y. Shyr and W. R. Ernst (*J. Catal.* **63**, 425 (1980)) were not successful until the adsorption kinetics appropriate to the system were used. The importance of properly describing the adsorption kinetics is emphasized and suggestions are offered when such data are not directly available.

INTRODUCTION

One common method for the preparation of highly dispersed metallic particles on oxidic supports is the incipient wetness technique. Here, the metallic dispersions are the result of impregnating the porous support with a liquid containing the catalytic ingredient, which is typically in the form of a dissolved salt. Small crystallites of the metal or compounds containing the catalytic metal are adsorbed on the internal surface of the support and both their size as well as the macroscopic distribution of metal within the support are determined by a large number of factors. The preparation variables and their influence on the distribution of active metals for a number of metal–support combinations have been investigated (*1–5*). The results of these studies have led to a body of knowledge of the physical and chemical processes of the impregnation process. Until recently this widely used method for producing commercial catalysts had very little fundamental basis. A more quantitative description of the impregnation process has been offered by Vincent and Merrill (*6*). They developed a single-pore model for one component adsorbing from solution. Their theoretical results were important because the critical factors that determine the profile of the impregnant within the catalyst pellet were defined. It was found that the concentration profile could be adjusted by the concentration of the catalyst in the solution or by controlling the temperature of impregnation. These facts are useful, for the optimum profile might be different depending on catalyst application. For example, for severely mass-transfer-controlled reactions, the optimum profile is a high catalyst loading near the pore mouth; while in the case of kinetically controlled reactions, the best results might be more aptly obtained with a uniform concentration profile.

Competitive Adsorption

The use of competitive adsorption as a means of controlling the concentration profile of active metal was first demonstrated by Maatman (*1*) for the case of platinum deposition from chloroplatinic acid on an alumina support. Uniform

0021-9517/81/060445-09$02.00/0

profiles of platinum could be obtained by adding HCl, HNO_3 or various inorganic nitrates to the impregnating solution.

The use of competitive adsorption to obtain a desired concentration profile has certain advantages over single-component adsorption:

(1) Vincent and Merrill (*6*) have shown how uniform profiles may be obtained for single-component adsorption. However, the minimum catalyst loading under which a uniform profile can be obtained is lower for the case of competitive adsorption than for single-component adsorption.

(2) With competitive adsorption, distributions other than "eggshell" or uniform can be obtained. The feasibility of this has been shown for HNO_3–$NiCl_2$ adsorption on γ-alumina spheres. By suitable choice of solution concentrations, Komiyama *et al.* (*7*) were able to generate a band of low-catalyst concentration at the pore mouth with higher concentration inside. Similar results have also been presented (*8*) for Pt impregnation onto alumina with a variety of coingredients.

The objective of this work was to extend the model calculations of Vincent and Merrill (*6*) to two competing ingredients in the impregnating solution. An earlier paper (*9*) had considered a model of multicomponent adsorption in which competing species diffused into a catalyst pellet prewetted with solvent. This choice was a direct result of the experimental procedure used to carry out the impregnation. We have chosen to follow the approach of Vincent and Merrill by modeling the process of catalyst impregnation as plug flow into a long cylindrical pore, (devoid of solvent), from a bulk solution of constant concentration. There were several reasons for adopting this model. Firstly, the numerical solutions for two-component adsorption could be readily compared and checked against the results given before (*6*). Secondly, our own experimental work in this area follows the more conventional impregnation of solution into a dried catalyst pellet, so that diffusive transport is negligible in the overall mass transfer. Since adsorption is rapid and since the nondimensionalized transport equations involve the ratios of adsorption rate parameters, we need not consider time explicitly. The effect of longer "impregnation times" when examined in the numerical solution is to increase the penetration depth of the profile into the catalyst pellet while still preserving the overall shape of the concentration profile.

For our choice of modeling, the effect of a number of controllable impregnation variables (solution concentration, etc.) on the resulting distribution have been identified. In our first modeling of the competitive coadsorption, we chose a simple Langmuir-type (site-available) description for the adsorption kinetics. We found that the model was not capable of reproducing earlier published results (*7, 8*). This has led us to the identification of perhaps the factor which most strongly effects the concentration distribution for the competitive coadsorption process: the coadsorption mechanism. From available data we will show that, in some instances, a detailed knowledge of the adsorption kinetics for each of the coingredients, can be melded into a description of the kinetics for the coadsorption. When this is done, reasonable agreement can be obtained between experimental and theoretical profiles.

In the sections to follow, we will first describe our model for the competitive adsorption of two species onto a support pellet using the idealized pore model and flow characteristics postulated by Vincent and Merrill (*6*). For this description we will assume simple Langmuir adsorption kinetics and identify the impregnation parameters which determine the characteristic concentration profiles. The effect of these parameters on the details of these profiles will then be discussed. We conclude this report by applying the competitive coadsorption model to the recent data of Shyr and Ernst (*8*). Here, the Langmuir-type kinetics will be modified to a form that is

more consistent with the data reported for the individual adsorption of the coingredients.

Before we begin our discussion it is important to emphasize that the objective here is to develop a model based on known or measured adsorption data for individual components and then *predict* the resulting distribution during coadsorption impregnation. This predictive quality is in contrast to the single-component adsorption treatment of existing profile data recently given (*7*).

Modeling

Vincent and Merrill (*6*) have modeled the process of catalyst impregnation as plug flow into a long cylindrical pore, from a bulk solution of constant concentration. The assumption of plug flow which is valid only for pores with a length to radius ratio $\gg 1$ removes the radial dependency of the mass transport equations. In addition, the effect of diffusion of the adsorbing species through the solution is assumed to be negligible. With these assumptions, the differential mass balance for the *i*th component can be written as

$$\frac{\partial \psi_i}{\partial \tau} + u \frac{\partial \psi_i}{\partial \Gamma} = - \frac{t_L}{c_{0i}} V_i (\psi_i, c_{0i}, \theta_i, \theta_j) \quad (1)$$

and

$$\frac{\partial \theta_i}{\partial \tau} = \frac{1}{c_s} V_i (\psi_i c_{0i}, \theta_i, \theta_j), \quad (2)$$

where

$$\begin{aligned} \psi_i &= c_i/c_{0i}; \\ \tau &= t/t_L; \\ \Gamma &= Z/L; \\ u &= \nu_p t_L/L. \end{aligned} \quad (3)$$

The notation of Vincent and Merrill (*6*) has been preserved as far as possible. In the above equations, c_i and c_{0i} are the local and bulk concentrations of species i, respectively; L is an arbitrary axial length along the cylindrical pore; t_L is the time required to reach a distance L; ν_p is the plug flow velocity, which may be a function of time t or of time and axial distance Z (*7*); u is the dimensionless velocity; the function V_i refers to the rate of adsorption of the *i*th component; c_s is the concentration of sites available for adsorption which is assumed to be a fixed quantity; and θ_i refers to the fraction of sites occupied by component i.

Since any tractable model of the catalyst impregnation process is necessarily idealized, the functional form chosen for ν_p is somewhat arbitrary. Based on Washburn's (*10*) empirically tested equation, Vincent and Merrill (*6*) have assumed that ν_p can be approximated as an infinite succession of Poiseuille steady states. Thus ν_p is a function of t only:

$$\nu_p = \frac{R}{4} \left(\frac{\Delta P}{\mu} \right)^{1/2} \cdot t^{1/2}, \quad (4)$$

where ΔP $(= 2\lambda/R)$ is a constant; λ is the surface tension of the solution; μ is the solution viscosity; and R is the pore radius. The functional form of V_i has been assumed to be given by first-order kinetics:

$$V_i = \frac{2k_{1i}}{R} c_i (1 - \Sigma \theta_j) - \frac{2k_{2i}}{R} \theta_i, \quad (5)$$

where k_{1i} refers to the adsorption rate constant and k_{2i} is the desorption constant for the i*th* species.

For a fixed set of parameters, the concentration profile has been found by us to depend strongly on the form of the competitive adsorption kinetics. However, it is useful to establish some general characteristics of the profiles based on a conventional (Langmuir-type) description of adsorption kinetics. Later we will show that single-component adsorption data can be utilized to predict concentration profiles when the assumption of Eq. (5) is no longer valid.

The numerical solution of Eqs. (1) and (2) along with Eqs. (4) and (5) is facilitated by introducing a new variable:

$$\tau^* = \tau^{1/2}; \quad (6)$$

and the final equations to be solved for the case of two-component adsorption on cata-

lyst supports are:

$$\frac{\partial \psi_i}{\partial \tau^*} = -\frac{\partial \psi_i}{\partial \Gamma} - 2\tau^* [K_{1i}\psi_i (1 - \theta_1 - \theta_2) - K_{2i}\theta_i], \quad (7)$$

$$\frac{\partial \theta_i}{\partial \tau^*} = 2\tau^* \left[\frac{K_{1i}}{\eta_i}\psi_i (1 - \theta_1 - \theta_2) - \frac{K_{2i}}{\eta_i}\theta_i\right], \quad (8)$$

where

$$K_{1i} = 2k_{1i}t_L/R, \quad K_{2i} = 2k_{2i}t_L/R\, c_{0i}, \quad \text{and } \eta_i = 2c_s/R\, c_{0i}. \quad (9)$$

The boundary conditions describing this problem are

$$\Gamma = 0, \quad \tau^* \geq 0; \ \psi_i = 1, \quad 0 \leq \Gamma \leq 1, \ \tau^* = 0; \ \theta_i = 0. \quad (10)$$

Equations (7) and (8) were solved by the GEARB routine (*11*), using the boundary conditions in Eq. (10), and a null boundary condition on the righthand side. Typical solution times were of the order of 1.5 min on the IBM 370 computer, and the equations were nonstiff, so the functional fixed-point iteration procedure was used for convergence. The axial length of $0 \leq \Gamma \leq 1$ was divided into 50 subsections and so 202 ODEs with a bandwidth of 8 were solved.

DISCUSSION

General

The concentration profiles θ_i versus Γ at $\tau = 1$ are shown in Figs. 1–6. The actual profiles can be interpreted in terms of a few simple parameters:

(1) Ratio of rate constants for single-species adsorption:

$$K_i' = \frac{K_{1i}\eta_i}{K_{2i}} = \frac{k_{1i}}{k_{2i}}\left(\frac{2c_s}{R}\right). \quad (11)$$

(2) Equilibrium value for single-species adsorption:

$$\theta_{i\max} = \frac{K_{1i}}{K_{1i} = K_{2i}} = \frac{K_i^*}{1 + K_i^*},$$

where

$$K_i^* = \frac{K_{1i}}{K_{2i}} = c_{0i}\frac{k_{1i}}{k_{2i}}. \quad (12)$$

(3) Ratio of rate constants for competitive adsorption:

$$K = \frac{K_1'}{K_2'} = \frac{k_{11}}{k_{21}} \times \frac{k_{22}}{k_{11}}. \quad (13)$$

(4) Equilibrium value for competitive adsorption:

$$\theta_{ieq} = \frac{K_i^*}{1 + K_1^* + K_2^*}. \quad (14)$$

(5) Bulk concentrations: c_{0i}

Parameters K_i' and K are characteristic of the given components and depend on the temperature. $\theta_{i\max}$ and θ_{ieq} depend on the concentrations c_{01} and c_{02} as well as on the temperature and the system. Thus in principle all these parameters can be varied experimentally. Komiyama, *et al.* (*7*) have studied the effect of bulk concentration on the adsorption of Ni on alumina from a solution containing $NiCl_2$ and HNO_3. Shyr and Ernst (*9*) have studied the effect of different coingredients on the concentration profile of Pt adsorbed on alumina pellets. Shyr and Ernst (*9*) have classified the observed catalyst concentration profiles into nine types. The nature of the concentration profile can be predicted by understanding the effects of the various parameters. The effect of these parameters is discussed in the next section for the competitive adsorption described by Eqs. (7) and (8). Later it will be shown that the experimental data of Shyr and Ernst (*8*) can be reconstructed by describing the competitive adsorption appropriate to the particular case.

Effect of Parameters

It was found that the concentration profiles θ_i versus Γ for a given time were basically sigmoidal and that each curve passed through a maximum either at the pore mouth or somewhere within the pore. The profiles at $\tau = 1.0$ can be interpreted in terms of three observations:

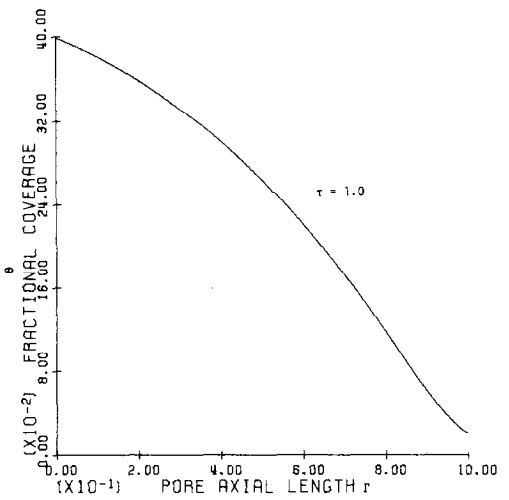

FIG. 1. Single-component adsorption, $K_{11} = K_{21} = 1$, $\eta_1 = 1.25$.

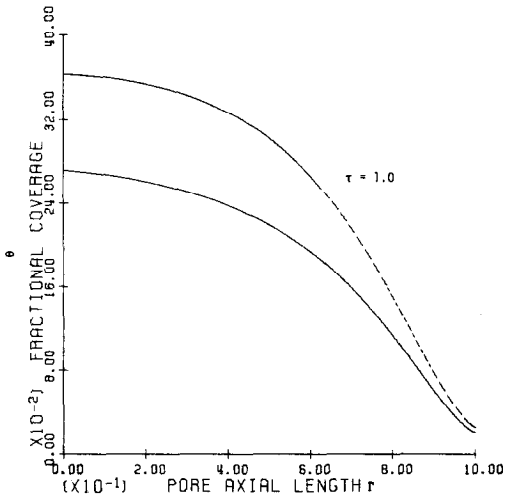

FIG. 2. Effect of slow-adsorbing coingredient. Solid curve represents species 1, while dashed curve represents species 2. Competitive adsorption parameters are $K_{11} = K_{21} = 1$, $\eta_1 = 1.25$, $K_{12} = K_{22} = 1.5$, $\eta_2 = 1.0$, $\theta_{1eq} = \theta_{2eq} = 0.333$, and $K = 1.25/1.0$.

(i) Deposition at the pore mouth: θ_{ieq} represents the equilibrium fractional coverage of component i at the pore mouth. Under competitive adsorption θ_i can never exceed the value θ_{imax}. However, depending on the relative rates of adsorption, it is possible for the fractional coverage at an arbitrary time to be greater than the equilibrium value θ_{ieq}. Specifically if $K > 1$; i.e., if $K_1' > K_2'$, the actual concentration θ_1 at the pore mouth approaches θ_{1eq} from below, while θ_2 approaches θ_{2eq} from above. This can be seen in Fig. 2, showing concentration profiles for the coingredients at $\tau = 1.0$. The reverse effect when $K < 1$ can be seen in Fig. 3.

(ii) Maximum fractional concentration: θ_{imax} is the maximum fractional concentration attainable by component i and can be achieved only when component i is in a noncompetitive situation. If θ_{ieq} is substantially less than θ_{imax}, it is possible for the profile of component i to pass through a maximum within the pore. This is shown for component 1 in Fig. 3.

(iii) Slope of the breakthrough: In every profile the concentration begins to decrease after some axial length. The slope of this breakthrough depends on concentration and on the value of K. For dilute solutions, the slope depends only on K. If $K < 1$, θ_1 falls off gradually while θ_2 decreases at a rapid rate. This can be seen in Fig. 3, while Fig. 2 shows a gradual breakthrough for both components ($K \approx 1$). At sufficiently high concentrations, however,

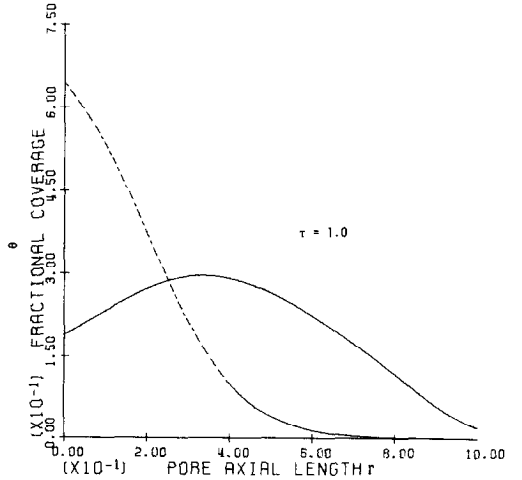

FIG. 3. Effect of fast-adsorbing coingredient. (——) species 1. (– – –) species 2. Parameters are $K_{11} = K_{21} = 1$, $\eta_1 = 1.25$, $K_{12} = 10$, $K_{22} = 1.5$, $\eta_2 = 5.0$, $\theta_{1eq} = 0.115$, $\theta_{1max} = 0.5$, $\theta_{2eq} = 0.769$, and $K = 1.25/33.3$.

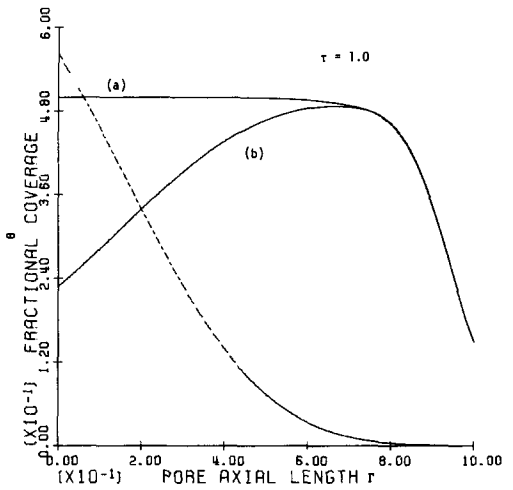

FIG. 4. Effect of fast-adsorbing coingredient on a concentrated bulk solution of species 1. Solid curve (a) is concentration profile of species 1 under single-component adsorption with parameters $K_{11} = K_{12} = 1$, $\eta_1 = 0.125$. Solid curve (b) is profile of species 1 obtained when coingredient (---) is added. Additional competitive adsorption parameters are $K_{12} = 10$, $K_{22} = 1.5$, $\eta_2 = 5.0$, $\theta_{1eq} = 0.115$, $\theta_{1max} = 0.5$, $\theta_{2eq} = 0.769$, and $K = 0.125/33.3$.

the pore can be saturated almost until $\Gamma = 1$. Fig. 4 shows the corresponding sharp breakthrough for the case of both single-component and multicomponent adsorption. As pointed out by Vincent and Merrill (*6*), the position of this sharp breakthrough depends on the bulk concentration.

While the actual concentration profile must still be obtained from the numerical solution, these three observations make it easier to predict the nature of the concentration profile and the effect of changing the system variables. For example, to produce a band of species 1 just within the pore, θ_{1eq} should be substantially lower than θ_{1max} and also K should be less than 1 so that species 2 falls off rapidly. The types of concentration profiles obtained with different systems and bulk concentrations are further discussed below.

Design of Catalyst Concentration Profiles

In the following discussion species 1 is assumed to be the catalytic ingredient:

Figure 1 shows the concentration profile of species 1 which is slow adsorbing and at dilute bulk concentration in a pure solution. Figure 2 shows that the adsorption of species 1 is suppressed by adding a slow-adsorbing species (species 2) at the same concentration level. Figure 3 shows the concentration profiles obtained when species 2 is a fast-adsorbing species at low bulk concentration. The presence of species 2 suppresses the concentration of species 1 at the pore mouth while the concentration within the pellet increases. A similar chromatographic separation can be seen in Fig. 4, where a fast-adsorbing species at low bulk concentration has been added to a solution containing a high concentration of slow-adsorbing species 1.

Comparing Figs. 3 and 5 shows the effect of increasing the concentration of species 1 by a factor of 10 in a competitive adsorption situation. The changes in the profiles can be understood in terms of the observations made in the last section. These observations can also be used to study the special case of irreversible adsorption. Figure 6 shows the concentration profile of species 1

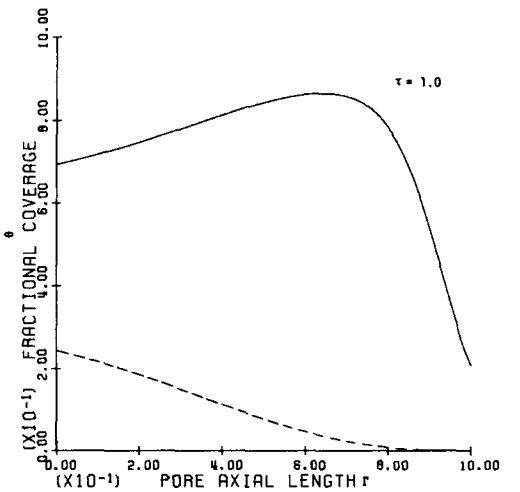

FIG. 5. Effect of increasing bulk concentration of species 1; comparison with Fig. 3. (———) species 1, (---) species 2. Parameters are $K_{11} = 1$, $K_{21} = 0.1$, $\eta_1 = 0.125$, $K_{12} = 10$, $K_{22} = 1.5$, $\eta_2 = 5.0$, $\theta_{1eq} = 0.566$, $\theta_{1max} = 0.909$, $\theta_{2eq} = 0.377$, and $K = 1.25/33.3$.

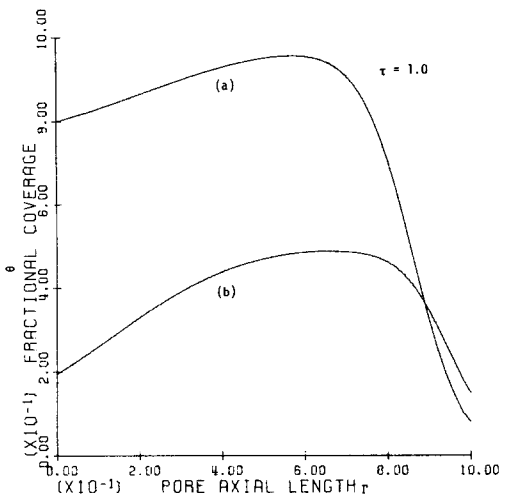

FIG. 6. Concentration profile of species 1 under irreversible adsorption. Curve (a) corresponds to $K_{11} = 1$, $K_{21} = 1.5$, $\eta_1 = 0.125$, $K_{12} = 10$, $K_{22} = 0$, $\eta_2 = 5.0$, $\theta_{1eq} = 0$, $\theta_{1max} = 0.5$, and $\theta_{2eq} = 1.0$. Curve (b) corresponds to $K_{11} = 1$, $K_{21} = 0$, $\eta_1 = 0.125$, $K_{12} = 10$, $K_{22} = 0$, $\eta_2 = 5.0$, $\theta_{1eq} = 0.8$, $\theta_{1max} = 1.0$, and $\theta_{2eq} = 0.2$.

when $K_{22} = 0$ and also when both K_{21} and $K_{22} = 0$. In the latter case

$$\theta_{1eq} = K_{11}\eta_2/(K_{11}\eta_2 + K_{12}\eta_1) = 1 - \theta_{2eq}. \quad (15)$$

The Effect of Competitive Coadsorption Kinetics on Catalyst Concentration Profiles

The preceding analysis has been based on the case where the two species competed for the same number of total sites on the catalyst support under first-order kinetics. As a result, the analysis has been simple and the effect of the various parameters can be easily delineated. The success of this approach as a predictive tool, however, depends critically on how well the competitive adsorption process is described by Eq. (5).

Shyr and Ernst (*8*) have studied the effect of adding various coingredients on the concentration profile of Pt adsorbing from a hexachloroplatinic acid solution onto γ-alumina pellets. They have also reported pure-component adsorption data for the case of citric acid (CA). From the adsorption isotherms of Pt and CA, it is apparent that the saturation coverage (μmoles/g) of CA is twice as large as that of Pt. Also the Pt isotherm can be fitted to the Langmuir model, which is not possible for CA. Based on these reported results we can postulate the following adsorption mechanism:

$$\text{Pt} + \text{site} \rightleftharpoons (\text{Pt} - \text{site}),$$
$$\text{CA} + \tfrac{1}{2}\,\text{site} \rightleftharpoons (\text{CA} - \tfrac{1}{2}\,\text{site}).$$

Let subscript 1 refer to Pt and subscript 2 to CA. Define

$$\theta_1 = q_1/c_s, \quad (0 < \theta_1 < 1), \quad (16)$$

$$\theta_2 = q_2/c_s, \quad (0 < \theta_2 < 2), \quad (17)$$

where c_s is the saturation coverage of Pt, while q_1 and q_2 are the amounts adsorbed. The competitive adsorption process may then be described as

$$\frac{\partial\theta_1}{\partial\tau^*} = 2\tau^* \left[\frac{K_{11}}{\eta_1}\psi_1 (1 - \theta_1 - \gamma\theta_2) - \frac{K_{21}}{\eta_1}\theta_1\right], \quad (18)$$

$$\frac{\partial\theta_2}{\partial\tau^*} = 2\tau^* \left[\frac{K_{12}}{\eta_2}\psi_2 (1 - \theta_1 - \gamma\theta_2)^{1/2} - \frac{K_{22}}{\eta_2}\theta_2\right]. \quad (19)$$

Equations (18) and (19) have been obtained in the same manner as Eq. (8). The variable γ has been introduced because upto 2 CA molecules can occupy one site. Hence γ can vary from 1 (at low coverages) to $\frac{1}{2}$ (at high coverages). A linear relationship between γ and θ_2 was assumed. The values of the various parameters can be calculated from the data of Shyr and Ernst (*8*):

$$\eta_i = 0.06518/c_{0i}(\text{M}); \quad (20)$$

$$K_{1i}/K_{2i} \approx 1330\, c_{0i}(\text{M}). \quad (21)$$

Only the values of K_{11} and K_{12} were not available, they were assumed to be 1.0 and 20.0, respectively. In principle these values are obtainable from a dynamic adsorption experiment. Figure 7 shows the predicted

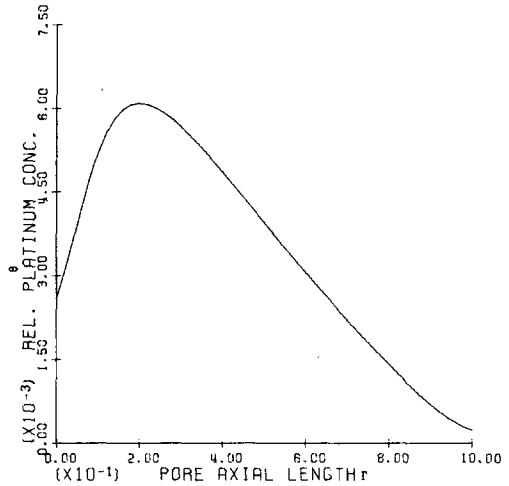

FIG. 7. Concentration profile of Pt using a dilute solution of coingredient at $\tau = 1.0$. $c_{01} = 5.65 \times 10^{-3}$ M, $c_{02} = 0.01$ M.

concentration profile of Pt when $c_{02} = 0.01$ M and $c_{01} = 5.65 \times 10^{-3}$ M. The predicted profile at $\tau = 1$ agrees well with the short-time observation of Shyr and Ernst (Table 1 of Ref. (*8*)). Figure 8 shows the predicted profile of Pt at $\tau = 0.45$, 0.63, and 0.78 when the bulk concentrations are $c_{02} = 0.03$ M and $c_{01} = 5.65 \times 10^{-3}$ M. The trend of the predicted profiles is consistent with the long-term profile observed by Shyr and Ernst (Fig. 6 of Ref. (*8*)).

CONCLUSIONS

The feasibility of predicting concentration profiles obtained from two-component competitive adsorption, using only single-component adsorption data, has been shown, in principle. The competitive adsorption model can also be used to predict the effect of changing process variables such as bulk concentrations and coingredients on the catalyst concentration profile. The prediction of concentration profiles can be improved by paying closer attention to the role of site utilization in the competitive process. For example, the data of Komiyama *et al.* (*7*) indicate that HNO_3 inhibits Ni adsorption to a degree larger than can be explained by a simple blocked-site type of mechanism. Replacement of catalyst by coingredient or poisoning of adjacent sites may be some phenomena that need to be incorporated into Eq. (5), which describes the kinetics of the coadsorption.

APPENDIX: NOMENCLATURE

- c_i Concentration of species i in solution phase
- c_s Adsorption capacity per unit area of pore wall
- c_{0i} Bulk concentration of species i
- k_{1i} Adsorption rate constant of species i, cm/sec
- k_{2i} Desorption rate constant of species i, moles/cm^2 · sec
- K_{1i} Reduced adsorption constant [Eq. (9)]
- K_{2i} Reduced desorption constant [Eq. (9)]
- K_i' Ratio of adsorption and desorption constants for the ith species [Eq. (11)]
- K_i^* Dimensionless Langmuir equilibrium parameter for species i [Eq. (12)]

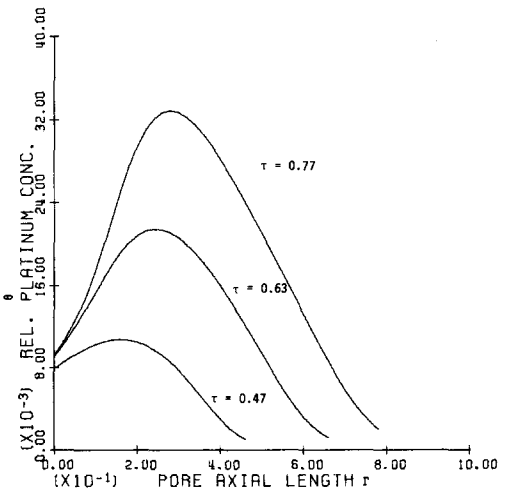

FIG. 8. Development of concentration profile of Pt using a concentrated solution of coingredient. $c_{01} = 5.65 \times 10^{-3}$ M, $c_{02} = 0.03$ M.

K Ratio of adsorption constants for competitive adsorption [Eq. (13)]
L Pore length
R Pore radius
t Time
t_L Time required to fill pore upto length L
u Reduced velocity [Eq. (3)]
ν_p Plug flow velocity
V_i Rate of removal of the ith species from solution
Z Axial position
Γ Reduced axial position [Eq. (3)]
η_i Relative adsorption capacity for the ith species
θ_i Fraction of sites occupied by species i
θ_{ieq} Equilibrium fractional coverage of species i
θ_{imax} Maximum fractional coverage of species i
λ Solution surface tension
μ Solution viscosity
τ Reduced time [Eq. (3)]
τ^* Square root of reduced time [Eq. (6)]
ψ Reduced concentration [Eq. (3)]
ΔP Constant pressure drop

ACKNOWLEDGMENTS

The authors thank Dr. J. Heydweiller for his assistance in obtaining the numerical solutions. We also wish to thank the editor for calling our attention to Ref. (9).

REFERENCES

1. Maatman, R. W., *Ind. Eng. Chem.* **51**(8), 913 (1959).
2. Cervello, J., Gardia de la Banda, J. F., Hermana, E., and Jimenez, J. F., *Chem. Eng. Technol.* **48**, 520 (1976).
3. Chen, H. C., and Anderson, R. B., *Ind. Eng. Chem. Prod. Res. Develop.* **12**(2), 122, (1973).
4. Santacesaria, E., Galli, C., and Carra, S., *React. Kinet. Catal. Lett.* **6**(3), 301 (1977).
5. Summers, J. C., and Hegedus, L. L., *J. Catal.* **51**, 185 (1978).
6. Vincent, R. C., and Merrill, R. P., *J. Catal.* **35**, 206 (1974).
7. Komiyama, M., Merrill, R. P., and Harnsberger, H. F., *J. Catal.* **63**, 35 (1980).
8. Shyr, Y., and Ernst, W. R., *J. Catal.* **63**, 425 (1980).
9. Hegedus, L. L., Chou, T. S., Summers, J. C., and Potter, N. M., "Preparation of Catalysts II," p. 171. Elsevier, Amsterdam, 1979.
10. Washburn, F. W., *Phy. Rev.* **17**(3), 273 (1921).
11. Madsen, N. K., and Sincovec, R. F., *Commun. Assoc. Comput. Mach.* (1973).